ARTICLE OPEN ACCESS

# Topographic Distribution of Amyloid-β, Tau, and Atrophy in Patients With Behavioral/Dysexecutive Alzheimer Disease

Joseph Therriault, BSc, Tharick A. Pascoal, MD, PhD, Melissa Savard, MSc, Andrea L. Benedet, PhD, Mira Chamoun, PhD, Cecile Tissot, BSc, Firoza Lussier, BSc, Min Su Kang, BSc, Emilie Thomas, PhD, Tatsuhiro Terada, MD, PhD, Soham Rej, MD, MSc, Gassan Massarweh, PhD, Ziad Nasreddine, MD, FRCPC, Paolo Vitali, MD, PhD, Jean-Paul Soucy, MD, MSc, Paramita Saha-Chaudhuri, PhD, Serge Gauthier, MD, FRCPC, and Pedro Rosa-Neto, MD, PhD

**Correspondence**
Dr. Rosa-Neto
pedro.rosa@mcgill.ca

*Neurology*® 2021;96:e81-e92. doi:10.1212/WNL.0000000000011081

## Abstract

### Objective

To determine the associations between amyloid-PET, tau-PET, and atrophy with the behavioral/dysexecutive presentation of Alzheimer disease (AD), how these differ from amnestic AD, and how they correlate to clinical symptoms.

### Methods

We assessed 15 patients with behavioral/dysexecutive AD recruited from a tertiary care memory clinic, all of whom had biologically defined AD. They were compared with 25 patients with disease severity– and age-matched amnestic AD and a group of 131 cognitively unimpaired (CU) elderly individuals. All participants were evaluated with amyloid-PET with [$^{18}$F] AZD4694, tau-PET with [$^{18}$F]MK6240, MRI, and neuropsychological testing.

### Results

Voxelwise contrasts identified patterns of frontal cortical tau aggregation in behavioral/dysexecutive AD, with peaks in medial prefrontal, anterior cingulate, and frontal insular cortices in contrast to amnestic AD. No differences were observed in the distribution of amyloid-PET or atrophy as determined by voxel-based morphometry. Voxelwise area under the receiver operating characteristic curve analyses revealed that tau-PET uptake in the medial prefrontal, anterior cingulate, and frontal insular cortices were best able to differentiate between behavioral/dysexecutive and amnestic AD (area under the curve 0.87). Voxelwise regressions demonstrated relationships between frontal cortical tau load and degree of executive dysfunction.

### Conclusions

Our results provide evidence of frontal cortical involvement of tau pathology in behavioral/dysexecutive AD and highlight the need for consensus clinical criteria in this syndrome.

From the Translational Neuroimaging Laboratory, The McGill University Research Centre for Studies in Aging, Douglas Hospital (J.T., T.A.P., M.S., A.L.B., M.C., C.T., F.L., M.S.K., E.T., T.T., P.V., S.G., P.R.-N.), and Departments of Neurology and Neurosurgery (J.T., T.A.P., A.L.B., M.C., C.T., F.L., M.S.K., E.T., P.V., J.-P.S., S.G., P.R.-N.), Psychiatry (S.R., S.G.), Radiochemistry (G.M.), and Epidemiology and Biostatistics (P.S.-C.), McGill University; Montreal Neurological Institute (J.T., T.A.P., A.L.B., M.C., C.T., F.L., M.S.K., G.M., J.-P.S., P.R.-N.), Canada; Department of Biofunctional Imaging (T.T.), Hamamatsu University School of Medicine, Japan; and MoCA Clinic and Institute (Z.N.), Montreal, Canada.

Go to Neurology.org/N for full disclosures. Funding information and disclosures deemed relevant by the authors, if any, are provided at the end of the article.
The Article Processing Charge was funded by Canadian Institutes for Health Research.

## Glossary

**Aβ** = Amyloid-β; **AD** = Alzheimer disease; **ADNI** = Alzheimer's Disease Neuroimaging Initiative; **AUC** = area under the receiver operating characteristic curve; **bvFTD** = behavioral variant frontotemporal dementia; **CDR** = Clinical Dementia Rating; **CU** = cognitively unimpaired; **lvPPA** = logopenic variant of primary progressive aphasia; **MMSE** = Mini-Mental State Examination; **PVC** = partial volume correction; **RFT** = random field theory; **ROC** = receiver operating characteristic; **SUVR** = standardized uptake value ratio; **VBM** = voxel-based morphometry.

The transition towards a biological definition of Alzheimer disease (AD)[1–3] has paved the way for the recognition of diverse clinical syndromes associated with AD pathology rather than the traditional conception of AD as an amnestic-predominant clinical syndrome.[4] Autopsy studies provide evidence that focal cortical syndromes such as posterior cortical atrophy and logopenic primary progressive aphasia can result from AD pathology.[5] Recent in vivo molecular imaging studies have extended this concept by providing evidence that the distribution of tau pathology is more closely related to clinical presentation than Amyloid-β (Aβ).[6,7]

The behavioral/dysexecutive variant of AD is characterized by predominant behavioral disinhibition, apathy, stereotyped behaviors, or executive dysfunction on cognitive testing.[3] Whereas behavioral/dysexecutive AD is attributable to AD pathophysiology, differential diagnosis from behavioral variant frontotemporal dementia remains a challenge because of overlapping clinical symptoms.[8] Autopsy studies assessing the distribution of Aβ and tau in behavioral/dysexecutive AD are small ($n \leq 6$) and report conflicting results.[9–11] Subsequent larger studies did not identify substantial frontal atrophy,[8,12] leading to the designation of "behavioral/dysexecutive AD" over "frontal variant AD." [8] However, these larger studies have not assessed the distribution Aβ or tau pathology,[8,12] which could be related to clinical presentation and anticipate focal neurodegeneration in these individuals.[13]

We aimed to assess the topographic distribution of Aβ and tau pathology in living patients with behavioral/dysexecutive AD. Building on recent molecular imaging studies,[14] we hypothesized that tau pathology will be found in frontal regions in behavioral/dysexecutive AD.

## Methods

### Participants

A study flowchart is presented in supplementary figure e-1 (data available from Dryad, doi.org/10.5061/dryad.rxwdbrv5m). We assessed cognitively impaired individuals with a clinical history compatible with behavioral variant frontotemporal dementia (bvFTD).[15] They had prominent behavioral or dysexecutive features in addition to amnestic symptoms and did not meet criteria for focal cortical syndromes such as primary progressive aphasia,[16] posterior cortical atrophy,[17] or other neurodegenerative diseases. These individuals were evaluated with physical and neurologic examinations by dementia specialists (T.A.P., Z.N., P.V., S.G., P.R.-N.) and neuropsychological evaluation by a neuropsychologist (E.T., P.V.). They also underwent Aβ PET with [$^{18}$F]AZD4694, tau PET with [$^{18}$F]MK6240, structural MRI, and genotyping for *APOEε4*. Ten of these individuals were deemed to not have AD following both negative amyloid-PET and tau-PET scans, and 1 individual was deemed to not have AD following a negative tau-PET scan despite having a positive amyloid-PET scan. Because these 11 individuals did not have biomarker evidence of AD,[1] they were excluded from the study. Based on their behavioral and executive dysfunction with relative preservation of other cognitive domains, the 15 remaining patients with biomarker evidence of AD (amyloid+/tau+) were classified as having behavioral/dysexecutive AD following a consensus meeting of dementia specialists and neuropsychologists. As consensus clinical criteria for this syndrome do not exist, we based our study's criteria on the criteria from the largest study on behavioral/dysexecutive AD[8] and subsequent studies that have also used these same methods,[12] with the additional criteria that participants had a clinical history compatible with possible bvFTD.[15] Of the 15 patients with amyloid+/tau+ behavioral/dysexecutive AD, 4 were referred to the memory center with a diagnosis of bvFTD, 3 were referred requesting a differential diagnosis of bvFTD vs frontal AD, 3 were referred with a diagnosis of "atypical dementia," 3 were referred with clinical diagnosis of AD with predominance of dysexecutive cognitive impairment, and 2 were referred with a clinical diagnosis of AD with predominance of behavioral changes. In this study we use the term "behavioral/dysexecutive AD" to refer to the spectrum of behavioral/dysexecutive presentations. [8] We also assessed cognitively unimpaired (CU) elderly ($n = 131$) and patients with amnestic AD ($n = 25$) who underwent Aβ PET with [$^{18}$F]AZD4694, tau PET with [$^{18}$F]MK6240, structural MRI, and genotyping for *APOEε4*. All participants had detailed clinical assessments including Mini-Mental State Examination (MMSE), Clinical Dementia Rating (CDR), and cerebrovascular disease risk with the Hachinski Ischemic Scale.[18] Apathy was assessed using the Apathy Inventory completed by the caregiver or study partner.[19] Assessment of amyloid and tau PET scans was done quantitatively (described in the Statistical methods section). CU elderly controls had a CDR of 0 and participants with AD had a CDR ≥ 0.5. Patients with amnestic AD met standard diagnostic criteria[20] for AD in addition to being positive for both Aβ and tau.[1] The amnestic AD group was age-matched

to help account for relationships between age and clinical presentation,[21] and matched for disease severity. Details of recruitment and clinical features of CU elderly and patients with amnestic AD are provided in reference 22.

## Standard Protocol Approvals, Registrations, and Patient Consents

This study's protocol was approved by McGill University's Institutional Review Board and informed written consent was obtained from all participants.

## Genetic Analyses

Determination of *APOE* genotypes was performed using the PCR amplification technique, followed by restriction enzyme digestion, standard gel resolution, and visualization processes. Full details of this procedure can be found elsewhere.[23]

## Neuropsychological Testing

Patients underwent a neuropsychological test battery that included evaluation of memory, language, and visuospatial and executive cognitive domains. Memory was assessed from the immediate and delayed logical memory as well as the Rey Auditory Verbal Learning immediate and delayed recall. Language was assessed with the Boston naming and category fluency tests. Visuospatial function was assessed with line orientation and copy tests of the Birmingham object recognition battery. Executive function was assessed using Trail-Making Test–B time, Digit Span Backward, and letter fluency (D words). Raw test scores were $z$ transformed using means and SDs from the same CU elderly population as used in neuroimaging comparisons (n = 131; table 1 for demographic and clinical information). Patient $z$ scores were averaged across all tests within each cognitive domain, resulting in a composite score for each domain.

## PET Image Acquisition and Processing

PET scans were acquired with a Siemens high-resolution research tomograph. [$^{18}$F]AZD4694 images were acquired 40–70 minutes postinjection and scans were reconstructed with the OSEM algorithm on a 4D volume with 3 frames (3 × 600 s). [$^{18}$F]MK6240 images were acquired 90–110 minutes postinjection and scans were reconstructed with the OSEM algorithm on a 4D volume with 4 frames (4 × 300 s).[24] Immediately following each PET acquisition, a 6-minute transmission scan was conducted with a rotating $^{137}$Cs point source for attenuation correction. The images underwent correction for dead time, decay, and random and scattered coincidences. T1-weighted images were nonuniformity and field-distortion corrected and processed using an in-house pipeline.[22] Then, PET images were automatically registered to the T1-weighted image space, and the T1-weighted images were linearly and nonlinearly registered to the *Alzheimer's Disease Neuroimaging Initiative*(*ADNI*) template space. Subsequently, a PET nonlinear registration was performed using the linear and nonlinear transformations from the T1-weighted image to the ADNI space and the PET to T1-weighted image registration. PET image partial volume correction (PVC) was carried out using the PETPVC toolbox.[25] Briefly, the region-based voxelwise correction technique was used to perform PVC using 10 tissue priors with a gaussian kernel with a full width at half maximum of 2.4 mm. The PET images were spatially smoothed to achieve a final resolution of 8 mm full-width at half maximum. All images were visually inspected to insure proper alignment to the ADNI template. [$^{18}$F]MK6240 standardized uptake value ratio (SUVR) maps were generated using the inferior cerebellar gray matter as a reference region and [$^{18}$F]AZD4694 SUVR maps were generated using the cerebellar gray matter as a reference region. A global [$^{18}$F]AZD4694 SUVR value was estimated for each participant by averaging the SUVR from the precuneus, prefrontal, orbitofrontal, parietal, temporal, anterior, and posterior cingulate cortices.[26]

## Structural MRI Acquisition and Processing

Structural MRI data were acquired at the Montreal Neurological Institute for all participants. Images were acquired on a 3T Siemens Magnetom using a standard head coil. A volumetric magnetization-prepared rapid gradient echo (MPRAGE) MRI (repetition time 2,300 ms, echo time 2.96 ms) sequence was employed to obtain a high-resolution T1-weighted anatomical image of the entire brain (9° flip angle, coronal orientation perpendicular to the double spin echo sequence, 1 × 1 mm$^2$ in-plane resolution of 1 mm slab thickness). T1-weighted anatomical images were segmented into probabilistic gray matter and white matter maps using the SPM12 segmentation tool. Each gray matter probability map was then nonlinearly registered (with modulation) to the ADNI template using DARTEL, voxel values were modulated by multiplying them by the Jacobian determinants derived from the spatial normalization step,[27] and images were smoothed with an 8 mm isotropic Gaussian kernel. All images were visually inspected to insure proper alignment to the ADNI template.

## Statistical Analyses

Baseline demographics were assessed using multiple $t$ tests and $\chi^2$ tests using the R Statistical Software Package version 3.3 (r-project.org/). To help circumvent potential biases related to visual classification of PET scans, we additionally used quantitative thresholds to assess positivity for both Aβ and tau. Amyloid-PET positivity was determined using an [$^{28}$F]AZD4694 SUVR threshold of 1.55 validated through gaussian mixture modeling, receiver operating characteristic (ROC) analyses, comparison with CSF biomarkers, and comparisons with young adults (age < 25).[28] All participants with AD had tau-PET SUVRs above the mean and 2 SD of the CU elderly group[29] in all Braak regions. Neuroimaging analyses were carried out using the VoxelStats toolbox (github.com/sulantha2006/VoxelStats), a MATLAB-based analytical framework

**Table 1** Demographic, Clinical, and Neuroimaging Characteristics of the Samples

| | CU | b/d AD | a AD | *p* Value (CU vs b/d AD) | *p* Value (CU vs a AD) | *p* Value (b/d AD vs a AD) |
|---|---|---|---|---|---|---|
| **No.** | 131 | 15 | 25 | — | — | — |
| **Age, y** | 68.2 (11.9) | 65.93 (8.75) | 65.83 (9.1) | 0.47 | 0.34 | 0.97 |
| **Female** | 87 (66) | 9 (60) | 12 (48) | 0.62 | 0.08 | 0.46 |
| **Education, y** | 15.19 (3.8) | 14.4 (3.4) | 14.56 (3.6) | 0.44 | 0.44 | 0.89 |
| ***APOE* ε4 carriers** | 42 (32) | 9 (60) | 15 (60) | 0.03 | 0.008 | 0.99 |
| **Apathy inventory** | 0.18 (0.52) | 7.6 (4.01) | 4.5 (3.11) | <0.0001 | <0.0001 | 0.009 |
| **MMSE** | 29.14 (1.2) | 19.6 (5.33) | 20.1 (5.7) | <0.0001 | <0.0001 | 0.78 |
| **Neocortical [$^{18}$F]AZD4694 SUVR** | 1.45 (0.39) | 2.36 (0.29) | 2.4 (0.43) | <0.0001 | <0.0001 | 0.75 |
| **Braak I–II [$^{18}$F]MK6240 SUVR** | 0.99 (0.29) | 1.94 (0.51) | 2.02 (0.86) | <0.0001 | <0.0001 | 0.75 |
| **Braak III–IV [$^{18}$F]MK6240 SUVR** | 1.04 (0.17) | 3.11 (1.09) | 2.89 (0.87) | <0.0001 | <0.0001 | 0.54 |
| **Braak V-VI [$^{18}$F]MK6240 SUVR** | 1.09 (0.13) | 3.06 (1.26) | 2.47 (0.96) | <0.0001 | <0.0001 | 0.1 |
| **Memory composite *z* score** | — | −2.53 (0.88) | −3.17 (0.97) | — | — | 0.04 |
| **Language composite *z* score** | — | −1.44 (0.92) | −1.48 (1.28) | — | — | 0.91 |
| **Visuospatial composite *z* score** | — | −1.25 (1.29) | −1.41 (1.16) | — | — | 0.69 |
| **Executive composite *z* score** | — | −3.52 (1.33) | −1.68 (1.15) | — | — | <0.0001 |

Abbreviations: a AD = amnestic Alzheimer disease; b/d AD = behavioral/dysexecutive Alzheimer disease; CU = cognitively unimpaired; MMSE = Mini-Mental State Examination; SUVR = standardized uptake value ratio.
Mean (SD) provided for continuous variables; number (%) for dichotomous variables. *p* Values indicate values assessed with 2-sided independent samples *t* tests for each variable except sex and *APOE ε4* status, where contingency $\chi^2$ tests were performed.

that allows for the execution of multimodal neuroimaging analyses in every brain voxel.

Voxelwise multivariate linear regression models were used to investigate the patterns of imaging biomarker abnormalities in behavioral/dysexecutive AD and amnestic AD as compared to CU elderly (n = 131). Each model was corrected for age as well as sex.[30] All voxelwise regression analyses were repeated using partial volume corrected PET data. Results were corrected for multiple comparisons using a random field theory (RFT)[31] cluster threshold of $p < 0.001$. An additional analytical step was performed to further investigate potential atrophy differences between groups, given potential heterogeneity of frontal atrophy reported in previous publications.[8] We generated mean and SD voxel-based morphometry (VBM) parametric maps based on the CU elderly population to create VBM *z* score maps for each patient with AD. VBM values that were greater than 1 SD from the mean were thresholded to create binary maps. The resulting voxelwise images show whether an individual's gray matter density falls outside the normal distribution of gray matter densities in the CU elderly population.[8] Next, frequency maps of thresholded voxels were generated in each clinical group.

To assess the accuracy of imaging biomarkers in differentiating between behavioral/dysexecutive and amnestic AD variants, we performed ROC analyses in every brain voxel to determine the area under the ROC curve (AUC) for each voxel. The optimal threshold value at every voxel was calculated using the least distance from a point to the ROC curve (0, 1; best operating point) contrasting behavioral/dysexecutive vs amnestic AD. This provides the best trade-off between sensitivity and specificity for differentiating between 2 categories, in this case, behavioral/dysexecutive vs amnestic AD. Next, we assessed the proportion of the frontal cortex differentially affected by Aβ, tau, and neurodegeneration in each clinical variant, assessed based on surpassing the optimal threshold of the ROC curve between behavioral/dysexecutive and amnestic AD.[32] Nonparametric *t* tests were used to compare the proportion of the frontal cortex differentially affected between behavioral/dysexecutive and amnestic AD groups.

Finally, we conducted voxelwise linear regressions between executive and memory composite *z* scores and tau-PET SUVR in the AD groups, correcting for age and sex. Results were also corrected for multiple comparisons using an RFT[31] cluster threshold of $p < 0.001$. [$^{18}$F]MK6240 SUVRs were extracted from significant clusters and displayed in scatterplots and density plots against composite *z* scores for each cognitive domain.

## Data Availability

Anonymized data and documentation from this study can be made available to qualified investigators on reasonable request. Such arrangements are subject to standard data sharing agreements.

# Results

## Demographics

Demographic, clinical, and neuroimaging information for all participants is summarized in table 1 (total n = 171). Both AD groups had higher neocortical [$^{18}$F]AZD4694 SUVR than CU elderly individuals, higher [$^{18}$F]MK6240 SUVR across all Braak regions, and lower MMSE scores. All patients with AD were positive for both amyloid and tau[1] based on quantitative thresholds. No differences in age, sex, education, MMSE score, APOE *ε4* carriership, or neocortical [$^{18}$F]AZD4694 SUVR were observed between AD groups. Patients with behavioral/dysexecutive AD had higher apathy scores than amnestic patients. All patients with AD had significantly impaired memory and executive function; patients with behavioral/dysexecutive AD had more severely impaired executive function relative to memory while amnestic patients with AD had more severe memory impairments relative to executive impairments. Supplementary table e-1 (data available from Dryad, doi.org/10.5061/dryad.rxwdbrv5m) summarizes the specific bvFTD criteria met by each patient with behavioral/dysexecutive AD. The most common bvFTD symptoms were loss of sympathy/empathy (14/15; 93%), followed by dysexecutive cognitive profile on neuropsychological testing with relative preservation of other cognitive domains (10/15; 66%) and behavioral disinhibition (10/15; 66%). Apathy or inertia were relatively frequent (9/15; 60%). Perseverative behaviors were only observed in 3 patients (3/15; 20%), and hyperorality was only observed in 1 advanced case.

## Amyloid, Tau, and Neurodegeneration in 15 Cases of Behavioral/Dysexecutive AD

Amyloid-PET, tau-PET, and T1-weighted MRI for each patient with behavioral/dysexecutive AD are presented in figure 1 accompanied by clinical and demographic information. Parametric SD maps for each imaging modality are reported in Supplementary figure e-2 (data available from Dryad, doi.org/10.5061/dryad.rxwdbrv5m).

## Voxelwise Regressions

Voxelwise linear regressions revealed that behavioral/dysexecutive AD and amnestic AD diagnoses were associated with similar patterns of [$^{18}$F]AZD4694 SUVR across the cerebral cortex compared with CU elderly (figure 2). Both groups displayed high [$^{18}$F]AZD4694 SUVR retention in posterior cingulate, precuneus, medial prefrontal, and lateral temporal cortices (RFT corrected, $p < 0.001$). Patients with amnestic AD had slightly elevated amyloid-PET uptake in medial prefrontal, inferior parietal, and occipital cortices, though the results did not survive correction for multiple comparisons. There were no brain regions in which patients with behavioral/dysexecutive AD had elevated [$^{18}$F]AZD4694 SUVR as compared to patients with amnestic AD. Results remained similar when using PVC data.

Voxelwise linear regressions revealed that behavioral/dysexecutive AD and amnestic AD diagnoses were associated with distinct patterns of [$^{18}$F]MK6240 SUVR across the cerebral cortex compared with CU elderly (figure 3). Patients with behavioral/dysexecutive AD had higher [$^{18}$F]MK6240 SUVR in the medial prefrontal, orbitofrontal, anterior cingulate, and frontal insular cortices. Patients with amnestic AD had a pattern of [$^{18}$F]MK6240 SUVR that was characterized by lateral temporal, inferior parietal, temporooccipital, posterior cingulate, and precuneus cortices. Both groups had high uptake in medial temporal, lateral temporal, and posterior cingulate cortices (RFT corrected, $p < 0.001$). Patients with behavioral/dysexecutive AD had elevated [$^{18}$F]MK6240 SUVR in the anterior cingulate, medial prefrontal, and frontal insula cortices compared to amnestic patients. Results remained similar when using PVC data.

Finally, voxelwise linear regressions revealed that behavioral/dysexecutive AD and amnestic AD diagnoses were associated with distinct patterns on VBM as compared with CU elderly individuals (figure 4). Similar to [$^{18}$F]MK6240 SUVR distribution, patients with amnestic AD had abnormalities in the lateral temporal, inferior parietal, temporooccipital, posterior cingulate, and precuneus cortices (RFT corrected at $p < 0.001$). When comparing patients with behavioral/dysexecutive AD with CU elderly, we observed VBM differences in the inferior parietal, posterior cingulate, precuneus, medial prefrontal, and dorsolateral prefrontal cortices (RFT corrected at $p < 0.001$). When comparing the 2 AD groups to each other, there were no group-level differences in regional brain atrophy. Frequency maps of brain atrophy are reported in Supplementary figure e-3 (data available from Dryad, doi.org/10.5061/dryad.rxwdbrv5m).

## Voxelwise ROC

To assess the accuracy of imaging biomarkers in differentiating between behavioral/dysexecutive and amnestic AD, we carried out ROC analyses in every brain voxel. Amyloid-PET uptake showed poor discriminative accuracy at distinguishing between behavioral/dysexecutive AD and amnestic AD (highest AUC ~60% across the cerebral cortex) (figure 5A). Voxelwise ROC analyses revealed that frontal [$^{18}$F]MK6240 uptake was able to discriminate between behavioral/dysexecutive AD and amnestic AD with high sensitivity and specificity (figure 5B). The highest AUCs were in the medial prefrontal cortex (AUC 87%), right frontal insula (AUC 82%), and anterior cingulate cortex (AUC 81%). VBM also showed poor ability to discriminate between behavioral/dysexecutive AD and amnestic AD (figure 5C). When comparing the percentage of frontal cortex differentially affected between groups, we did not observe differences in Aβ ($p = 0.46$) or VBM ($p = 0.81$). However, the percentage of frontal cortex differentially affected by tau was higher in the

**Figure 1** Amyloid-PET, Tau-PET, and T1-Weighted MRI for Each Patient with Alzheimer Disease (AD) with Behavioral/Dysexecutive Phenotype

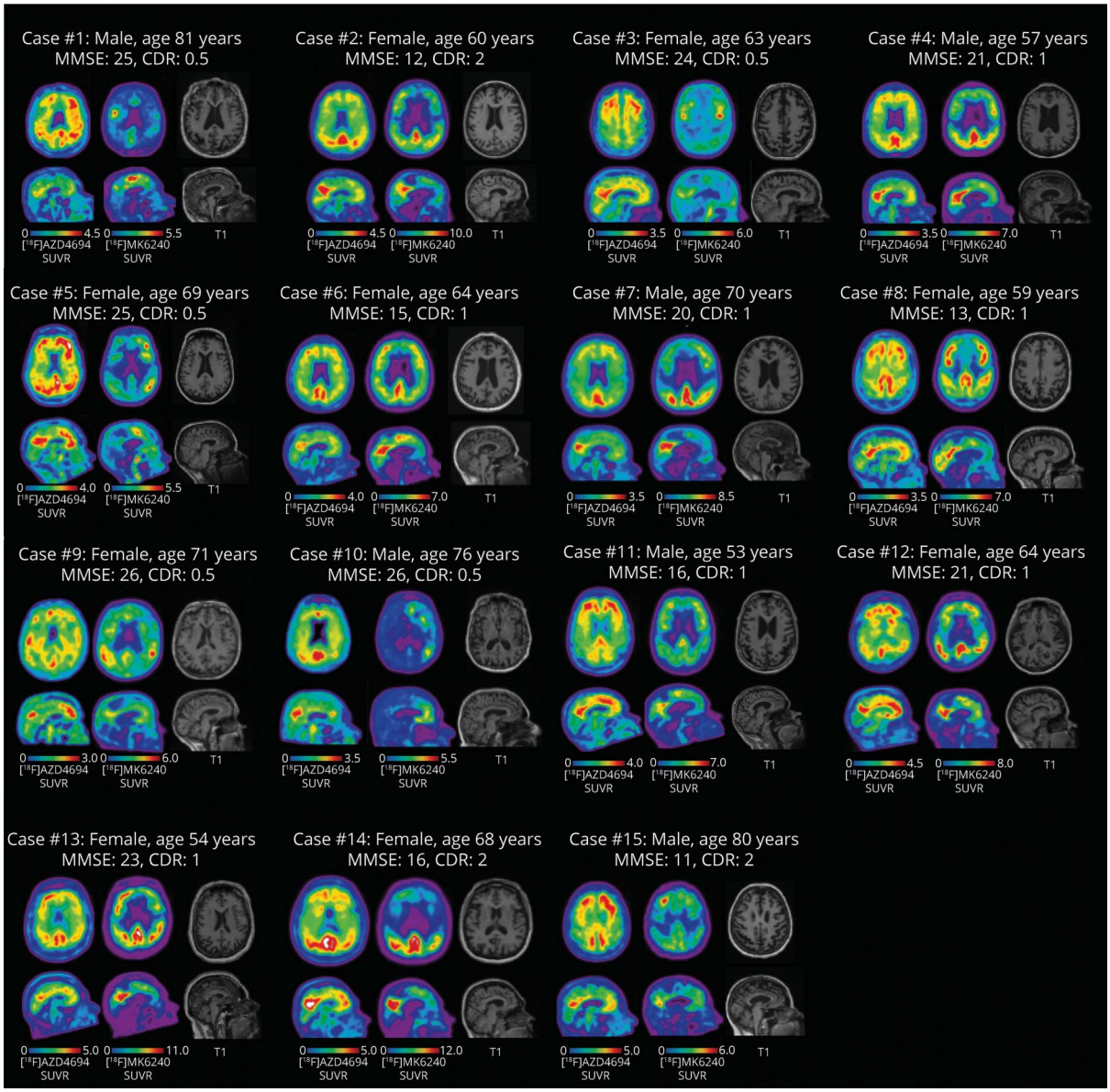


Axial (top row) and midsagittal (bottom row) slices for each patient with AD. Each patient is positive for amyloid and tau. Left column: [$^{18}$F]AZD4694 (amyloid-PET). Middle column: [$^{18}$F]MK6240 (tau-PET). Right column: T1-weighted MRI. CDR = Clinical Dementia Rating; MMSE = Mini-Mental State Examination; SUVR = standardized uptake value ratio.

behavioral/dysexecutive group compared to the amnestic AD group ($p = 0.006$).

## Neuropsychological Associations

Voxelwise analyses revealed significant relationships between executive function composite $z$ scores and [$^{18}$F]MK6240 SUVR in the anterior cingulate, orbitofrontal, medial prefrontal, and dorsolateral prefrontal cortices (RFT corrected at $p < 0.001$; β estimate −0.65, standard error 0.19) (figure 6A). Voxelwise analyses also revealed significant relationships between memory composite $z$ scores and [$^{18}$F]MK6240 SUVR in the lateral temporal, posterior cingulate, precuneus, and inferior parietal cortices (RFT corrected at $p < 0.001$; β estimate −0.33; standard error 0.11) (figure 6B). Results were similar when using PVC data.

# Discussion

In this study, we assessed the topographic distribution of Aβ, tau, and atrophy in patients with AD with prominent behavioral or dysexecutive clinical features. The main finding of our study is that behavioral/dysexecutive AD is associated with a set of distinct patterns of tau pathology in the frontal cortex. We did not observe regional associations between behavioral/dysexecutive AD and frontal Aβ or

**Figure 2** Topographic Distribution of Amyloid-β in Amnestic and Behavioral/Dysexecutive (b/d) Variants of Alzheimer Disease (AD)

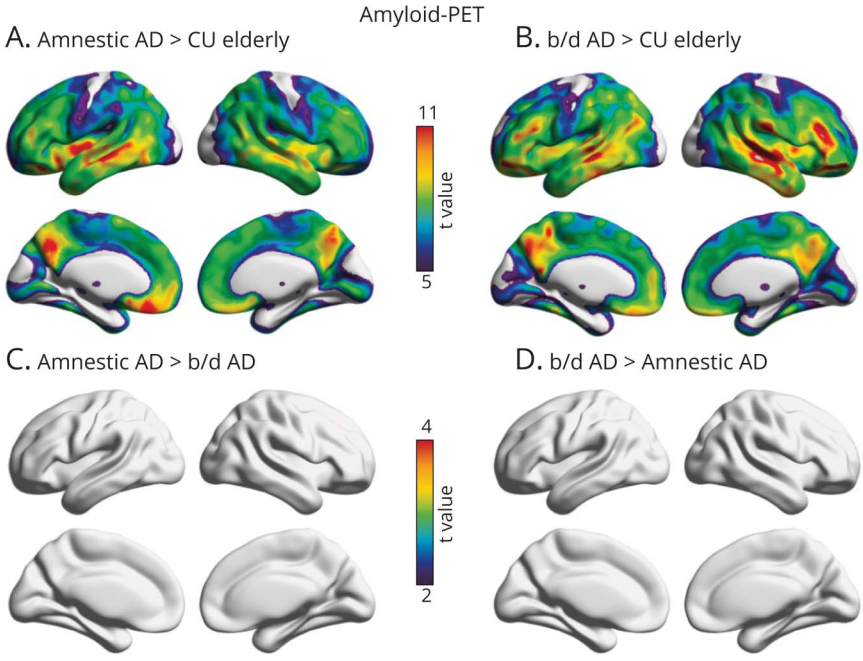


(A) Voxelwise regressions revealed that patients with amnestic AD had elevated amyloid-PET in the posterior cingulate, precuneus, inferior parietal, medial prefrontal, and occipital cortices as compared to cognitively unimpaired (CU) elderly. (B) Voxelwise regressions revealed that patients with behavioral/dysexecutive AD had elevated amyloid-PET in the posterior cingulate, precuneus, inferior parietal, and medial prefrontal cortices compared to CU elderly. (C, D) No differences in the topography of amyloid-PET were observed between patients with amnestic AD as compared to patients with behavioral/dysexecutive AD. *t* Statistical parametric maps were corrected for multiple comparisons using a random field theory cluster threshold of $p < 0.001$. Age and sex were employed as covariates in each model.

atrophy. Frontal tau pathology differentiated behavioral/dysexecutive vs amnestic AD variants and correlated with severity of executive dysfunction. Our results provide evidence of frontal involvement in behavioral/dysexecutive AD and contribute to a framework in which the anatomical distribution of tau pathology is closely related to clinical presentations of AD.[14]

The brain regions with the highest discriminative accuracy for a diagnosis of behavioral/dysexecutive AD vs amnestic AD

**Figure 3** Topographic Distribution of Amyloid-β in Amnestic and Behavioral/Dysexecutive (b/d) Variants of Alzheimer Disease (AD)

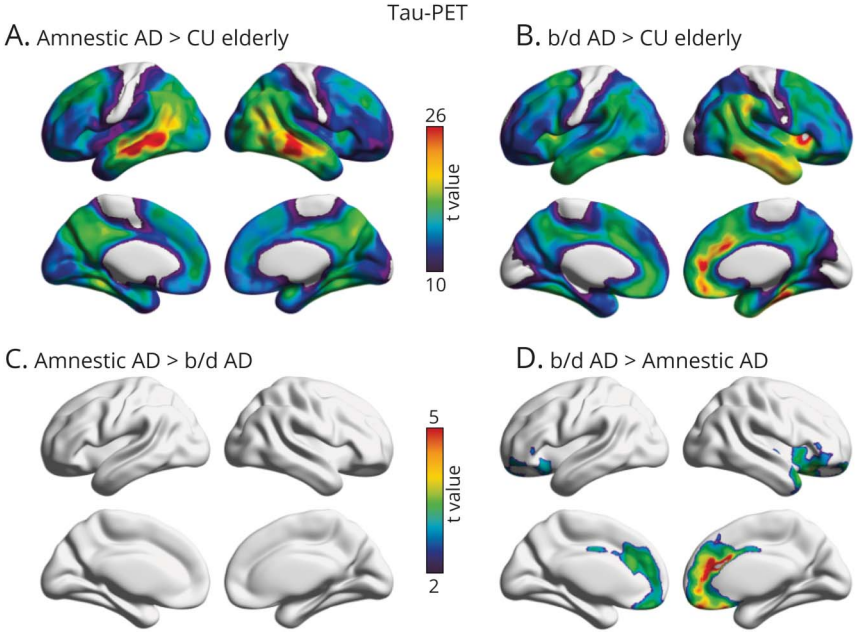


(A) Strongest associations between [$^{18}$F]MK6240 standardized uptake value ratio (SUVR) and amnestic AD were observed in lateral temporal, inferior parietal, precuneus, and posterior cingulate cortices. (B) Strongest associations between [$^{18}$F]MK6240 SUVR and behavioral/dysexecutive AD were observed in the anterior cingulate, lateral temporal, frontal insula, and orbitofrontal cortices. (C) *t* Maps displaying significant differences between patients with behavioral/dysexecutive AD and patients with amnestic AD; after multiple comparisons correction with random field theory ($p < 0.001$), no results remained significant. (D) *t* Maps displaying significant differences between patients with behavioral/dysexecutive AD and patients with amnestic AD. Behavioral/dysexecutive subjects had greater tau-PET uptake in medial prefrontal, anterior cingulate, and frontal insular cortices. *t* Statistical parametric maps were corrected for multiple comparisons using a random field theory cluster threshold of $p < 0.001$. Age and sex were employed as covariates in each model. CU = cognitively unimpaired.

**Figure 4** Topographic Distribution of Atrophy in Amnestic and Behavioral/Dysexecutive (b/d) Variants of Alzheimer Disease (AD)

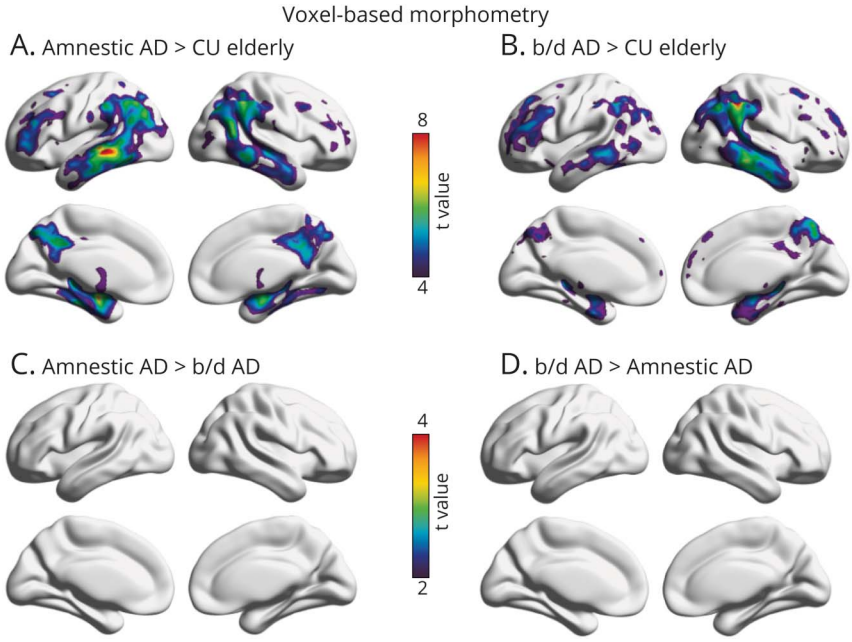


(A) Strongest associations between voxel-based morphometry (VBM) and amnestic AD were observed in lateral temporal, inferior parietal, precuneus, and posterior cingulate cortices. (B) Strongest associations between VBM and behavioral/dysexecutive AD were observed in the lateral temporal, inferior parietal, dorsolateral, and medial prefrontal cortices. (C, D) *t* Maps displaying no statistically significant differences between patients with behavioral/dysexecutive AD and amnestic AD. *t* Statistical parametric maps were corrected for multiple comparisons using a random field theory cluster threshold of $p < 0.001$. Age, sex, and Mini-Mental State Examination were employed as covariates in each model. CU = cognitively unimpaired.

were the medial prefrontal, anterior cingulate, and frontal insular cortices. The medial prefrontal cortex has been consistently implicated in emotional processing.[33] Evidence from single neuron recordings[34] as well as fMRI studies[35] have linked anterior cingulate cortex activity with complex decision-making and behavioral monitoring. Similarly, the frontal insular cortices are involved in the detection of behaviorally relevant stimuli to guide decision-making.[36] The anterior cingulate cortex and frontal insula are also affected in bvFTD,[37] which shares many symptoms with behavioral/dysexecutive AD. The anterior cingulate cortex and frontal insula are constituents of the brain's salience network,[38] also vulnerable in bvFTD.[39] A recent study has identified metabolic dysfunction in the frontal insula in patients with behavioral/dysexecutive AD compared to those with typical AD,[12] further corroborating the relationship between the brain's salience network and behavioral symptoms in neurodegenerative diseases including bvFTD and AD.

It has been proposed that the absence of a consistent pattern of frontal brain atrophy challenges the concept of "frontal AD."[8] In line with previous studies, we did not observe consistent patterns of frontal atrophy at the group level that differed from amnestic AD. This could be attributable to the substantial heterogeneity of atrophy in patients with behavioral/dysexecutive presentations in our sample. It is also possible that a more sensitive measure of neurodegeneration such as [$^{18}$F]FDG-PET may capture topographic differences in cortical neurodegeneration not observed in our study.[12] Longitudinal analysis may clarify atrophy patterns in behavioral/dysexecutive AD as neurodegeneration follows tau-PET uptake[13,40] and correlates with neurofibrillary tangle distribution at autopsy.[41]

Our study did not observe significant differences in cerebral Aβ distribution between behavioral/dysexecutive and amnestic variants of AD, in contrast to autopsy studies with smaller sample sizes ($n \leq 6$).[9,11] However, the lack of regional differences in Aβ deposition between AD variants agrees with previous reports of similar distributions of Aβ pathology when comparing amnestic AD and posterior cortical atrophy (PCA),[42] as well as comparisons between amnestic AD and logopenic variant of primary progressive aphasia (lvPPA).[43] These studies highlight the need for a better mechanistic understanding of cerebral tau propagation: in the face of similar Aβ pathology, why do variants of AD display tau aggregation in different regions? Case–control studies have suggested that individuals with PCA have a higher lifetime prevalence of visuospatial learning disabilities[44] and individuals with lvPPA are more likely to have language-related learning disabilities than healthy control individuals,[45] though without biomarker evidence it is unknown how many of these cases are due to AD. Overall, the finding of similar Aβ distribution across different AD clinical syndromes supports a framework in which Aβ deposition is an early but not sufficient factor in the pathogenesis of AD dementia.[1]

Early and accurate identification of AD pathophysiology is critical for clinical trial enrichment, diagnostic assessment, and increasingly, changes in clinical care.[46] While MRI, CSF, and amyloid-PET are being performed more frequently in the diagnosis and clinical management of

**Figure 5** Accuracy of Imaging Biomarkers for Discriminating Behavioral/Dysexecutive (b/d) Alzheimer Disease (AD) From Amnestic AD

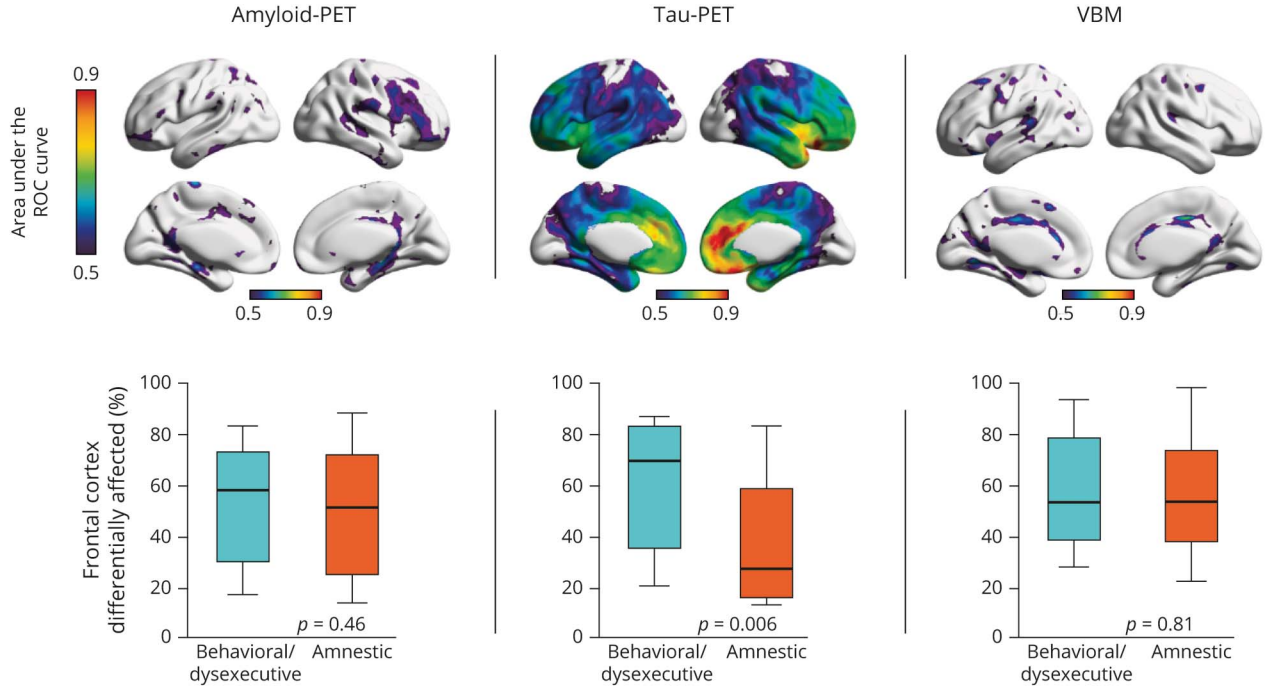


Top row: Area under the receiver operating characteristic (ROC) curve in every brain voxel for amyloid-PET (left), tau-PET (middle), and voxel-based morphometry (VBM) (right). Amyloid-PET showed poor discriminatory accuracy between behavioral/dysexecutive AD and amnestic AD. Area under the receiver operating characteristic curve (AUC) values for tau-PET varied substantially, with highest AUC values being observed in the medial prefrontal cortex, anterior cingulate cortex, and frontal insula, while lower values were observed in posterior cortical regions. Voxel-based morphometry demonstrated low discriminatory accuracy between behavioral/dysexecutive and amnestic AD groups. Bottom row: Percentage of frontal cortex differentially affected in behavioral/dysexecutive AD vs amnestic AD. No differences were observed in frontal cortical amyloid between AD groups ($p = 0.46$). Significant differences in frontal cortical tau-PET were observed between behavioral/dysexecutive and amnestic AD groups (p = 0.006). No significant differences were observed in frontal cortical voxel-based morphometry between AD groups (p = 0.81).

cognitive impairment, the clinical utility of tau-PET imaging is unknown. Our results suggest that tau-PET may have utility to both identify tau pathology in behavioral/dysexecutive AD as well as to distinguish behavioral/dysexecutive AD from amnestic AD and FTD, in line with a recent multicenter study demonstrating tau-PET's discriminative accuracy for the differential diagnosis of dementia syndromes.[47]

Despite that fact that frontal tau-PET uptake was able to discriminate between groups, we observed substantial variability in the topography of [$^{18}$F]MK6240 uptake in the behavioral/dysexecutive AD group. Numerous prefrontal cortical regions were affected across patients, providing neuroimaging support for potential dissociations between behavioral and dysexecutive subtypes of AD.[8] Variability in the topographic distribution of tau-PET uptake in this clinical syndrome suggests there may be limitations in selecting a single brain region to differentiate between clinical groups. It is also important to consider that multiple pathologies can be related to cognitive decline.[48] Positive biomarkers for AD do not exclude the presence of other neuropathologic comorbidities.[49] The issue of the heterogeneity in behavioral/dysexecutive AD is exacerbated by the lack of consensus clinical criteria for this syndrome, in contrast to other syndromes such as lvPPA[16] and PCA.[17]

An unanswered question is to what degree behavioral/dysexecutive AD constitutes a clinical entity separate from typical AD. While patients with behavioral/dysexecutive AD had greater executive impairment relative to other cognitive domains, both behavioral/dysexecutive and amnestic clinical phenotypes had high tau load in AD-related areas including lateral temporal, posterior cingulate, precuneus, and inferior parietal cortices.[50] Likewise, case reports of "frontal AD" typically describe significant behavioral or dysexecutive features in the context of amnestic impairment.[9–11] Longitudinal studies may clarify the extent to which behavioral, dysexecutive, and amnestic dysfunction (either together or in isolation) define this syndrome over time, and how this may differ from both amnestic AD and bvFTD.

Some methodologic limitations should be considered when interpreting our study. The most important limitation is the lack of consensus classification guidelines for behavioral/dysexecutive AD. Currently, classification of behavioral/dysexecutive AD is based on consensus judgement of a clinical team,[8,12] which can lead to variability between centers. This

**Figure 6** Association of Frontal Tau-PET Uptake With Executive Dysfunction in Alzheimer Disease (AD)

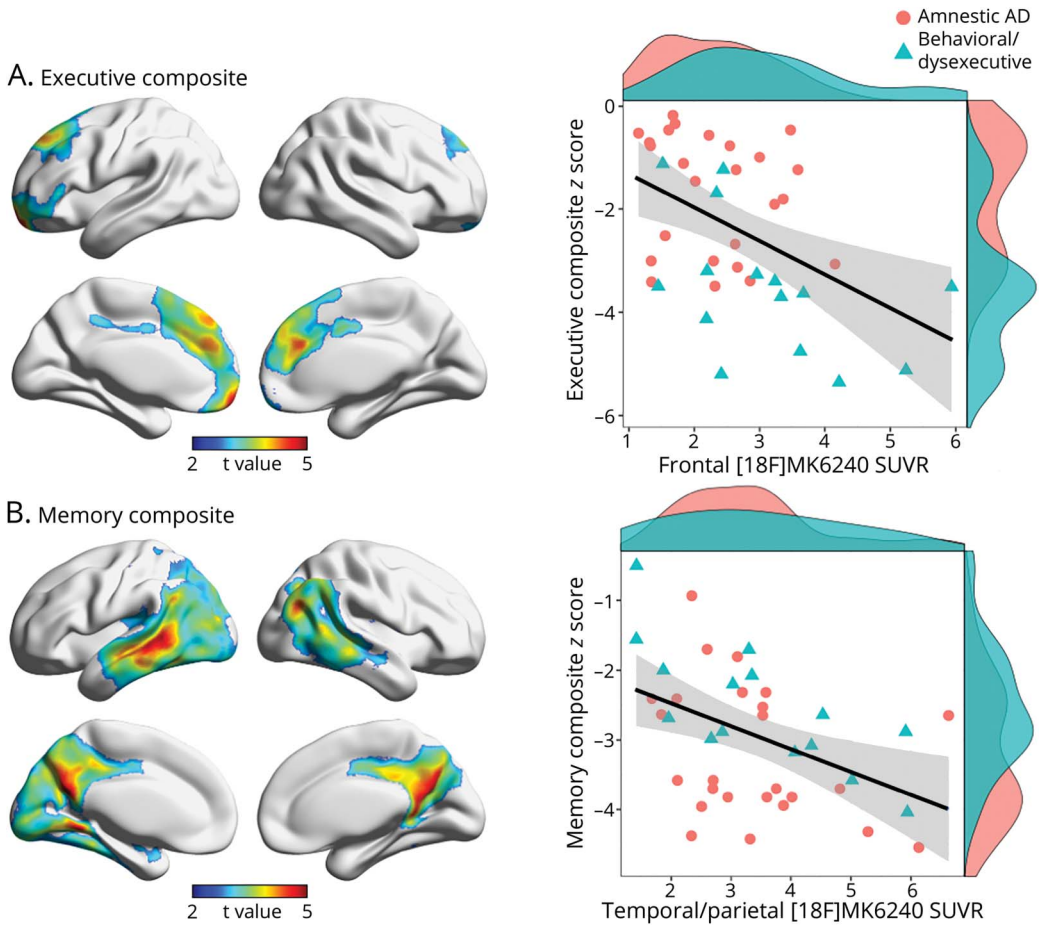


(A) Left: Statistically significant relationships between executive function composite *z* score and [$^{18}$F]MK6240 SUVR after multiple comparisons correction with random field theory at $p < 0.001$. Significant clusters were used to extract tau-PET (SUVR) values. Right: Scatterplots display associations between frontal cortical [$^{18}$F]MK6240 SUVR and executive function composite score (β estimate: −0.65, standard error: 0.19). (B) Left: Statistically significant relationships between memory composite *z* score and [$^{18}$F]MK6240 SUVR after multiple comparisons correction with random field theory at $p < 0.001$ (β estimate: −0.33, standard error: 0.11). Significant clusters were used to extract tau-PET SUVR values. Right: Scatterplots display associations between [$^{18}$F]MK6240 SUVR and memory composite *z* score. Density plots are provided along the x and y axes to visualize the distribution of [$^{18}$F]MK6240 SUVRs and cognitive function composite *z* scores, respectively. Age and sex were employed as covariates in each analysis.

stands in contrast to other focal cortical AD syndromes with established clinical and imaging guidelines such as lvPPA[16] and PCA.[17] In our study, all patients with behavioral/dysexecutive AD had a clinical history compatible with bvFTD.[15] While meeting existing standardized phenotypic criteria may help with reproducibility, this framework may have overlooked patients with predominant executive dysfunction without behavioral impairment described in previous publications,[8] in which lateral prefrontal tau-PET was associated with executive impairment.[51] Future work is needed to identify clinical criteria for behavioral/dysexecutive AD and to determine the potential role of imaging biomarkers in this classification scheme. Secondly, because the majority of patients in our study presented with both behavioral changes and executive dysfunction, we did not assess specific differences between the 2 subtypes, instead using the term behavioral/dysexecutive AD to refer to the spectrum of behavioral and dysexecutive presentations. [8] A related limitation is that the cases of behavioral/dysexecutive AD included in our study were relatively advanced (mean MMSE 19.6), rendering potential dissociations between behavioral and dysexecutive phenotypes difficult to ascertain. Future longitudinal studies with detailed behavioral and neuropsychological evaluations may inform the extent to which behavioral/dysexecutive AD constitutes a single entity or a clinical continuum.[8] Small sample size is another important limitation; however, our study is the largest in vivo molecular imaging study of behavioral/dysexecutive AD to date. Our sample is also taken from a tertiary care memory clinic comprising relatively young patients, which may limit generalizability.

We report that the behavioral/dysexecutive variant of AD is associated with a distinct topographic pattern of tau pathology in medial prefrontal, anterior cingulate, frontal insular, and orbitofrontal cortices. The degree of tau-PET uptake in

frontal regions was associated to the degree of executive dysfunction in these patients. Our results highlight the importance of imaging biomarkers for the differential diagnosis of cognitive impairment.


## Acknowledgment

The authors thank the participants of the study; the staff of the McGill Center for Studies in Aging for their role in data collection; Mallery Landry for help with patient recruitment; and Dean Jolly, Alexey Kostikov, Monica Samoila-Lactatus, Karen Ross, Mehdi Boudjemeline, and Sandy Li for their assistance with radiochemistry production.

## Study Funding

J. Therriault is funded by McGill University's Faculty of Medicine Student Scholarship. P. Rosa-Neto is supported by the Weston Brain Institute, the Canadian Institutes of Health Research (CIHR) (MOP-11-51-31, PR N), the Alzheimer's Association (NIRG-12-92090, NIRP-12-259245, PR-N), and Fonds de Recherche du Québec–Santé (FRQS; Chercheur Boursier, 2020-VICO-279314). T.A. Pascoal, P. Rosa-Neto, and S. Gauthier are members of the CIHR-CCNA Canadian Consortium of Neurodegeneration in Aging.


## Disclosure

The authors report no disclosures relevant to the manuscript. Go to Neurology.org/N for full disclosures.


## Publication History

Received by *Neurology* April 8, 2020. Accepted in final form August 12, 2020.


## Appendix Authors

| Name | Location | Contribution |
|---|---|---|
| **Joseph Therriault, BSc** | McGill University, Montreal, Quebec, Canada | Study concept and design, analysis and interpretation of data, creation of figures and manuscript draft |
| **Tharick Pascoal, MD, PhD** | McGill University, Montreal, Quebec, Canada | Study concept and design, analysis and interpretation of data, creation of figures and manuscript draft |
| **Andrea L. Benedet, PhD** | McGill University, Montreal, Quebec, Canada | Study concept and design, analysis and interpretation of data, creation of figures and manuscript draft |
| **Cecile Tissot, BSc** | McGill University, Montreal, Quebec, Canada | Study concept and design, analysis and interpretation of data, creation of figures and manuscript draft |
| **Melissa Savard, MSc** | McGill University, Montreal, Quebec, Canada | Study concept and design, analysis and interpretation of data, creation of figures and manuscript draft |
| **Mira Chamoun, PhD** | McGill University, Montreal, Quebec, Canada | Image data processing, analysis and interpretation of data, manuscript draft |
| **Firoza Lussier, BSc** | McGill University, Montreal, Quebec, Canada | Image data processing, analysis and interpretation of data, manuscript draft |
| **Min Su Kang, BSc** | McGill University, Montreal, Quebec, Canada | Image data processing, analysis and interpretation of data, manuscript draft |
| **Emilie Thomas, PhD** | McGill University, Montreal, Quebec, Canada | Neuropsychological data acquisition and file review, manuscript draft |
| **Soham Rej, MD, MSc** | McGill University, Montreal, Quebec, Canada | Critical revision of manuscript for intellectual content |
| **Tatsuhiro Terada, MD, PhD** | Hamamatsu University School of Medicine | Image data processing, analysis and interpretation of data, manuscript draft |
| **Ziad Nasreddine, MD, FRCPC** | McGill University, Montreal, Quebec, Canada | Critical revision of manuscript for intellectual content |
| **Jean-Paul Soucy, MD, MSc** | McGill University, Montreal, Quebec, Canada | Study supervision and critical review of manuscript for intellectual content |
| **Gassan Massarweh, PhD** | McGill University, Montreal, Quebec, Canada | Study supervision and critical review of manuscript for intellectual content |
| **Paolo Vitali, MD, PhD** | McGill University, Montreal, Quebec, Canada | Study supervision and critical review of manuscript for intellectual content |
| **Paramita Saha-Chaudhuri** | McGill University, Montreal, Quebec, Canada | Study concept, design, analysis and interpretation of data, creation of figures and manuscript draft |
| **Serge Gauthier, MD, FRCPC** | McGill University, Montreal, Quebec, Canada | Study supervision and critical review of manuscript for intellectual content |
| **Pedro Rosa-Neto, MD, PhD** | McGill University, Montreal, Quebec, Canada | Study concept, design, analysis and interpretation of data, creation of figures and manuscript draft |

## References


1. Jack CR, Bennett DA, Blennow K, et al. NIA-AA Research Framework: toward a biological definition of Alzheimer's disease. Alzheimers Dement 2018;14:535–562.
2. McKhann GM, Knopman DS, Chertkow H, et al. The diagnosis of dementia due to Alzheimer's disease: recommendations from the National Institute on Aging-Alzheimer's Association workgroups on diagnostic guidelines for Alzheimer's disease. Alzheimers Dement 2011;7:263–269.
3. Dubois B, Feldman HH, Jacova C, et al. Advancing research diagnostic criteria for Alzheimer's disease: the IWG-2 criteria. Lancet Neurol 2014;13:614–629.
4. Knopman DS, Petersen RC, Jack CR. A brief history of "Alzheimer disease": multiple meanings separated by a common name. Neurology 2019;92:1053–1059.
5. Alladi S, Xuereb J, Bak T, et al. Focal cortical presentations of Alzheimer's disease. Brain 2007;130:2636–2645.
6. Ossenkoppele R, Smith R, Ohlsson T, et al. Associations between tau, Aβ, and cortical thickness with cognition in Alzheimer disease. Neurology 2019;92:e601–e612.
7. Lowe VJ, Bruinsma TJ, Wiste HJ, et al. Cross-sectional associations of tau-PET signal with cognition in cognitively unimpaired adults. Neurology 2019;93:e29–e39.
8. Ossenkoppele R, Pijnenburg YA, Perry DC, et al. The behavioral/dysexecutive variant of Alzheimer's disease: clinical, neuroimaging and pathological features. Brain 2015;138:2732–2749.
9. Taylor KI, Probst A, Miserez AR, Monsch AU, Tolnay M. Clinical course of neuropathologically confirmed frontal-variant Alzheimer's disease. Nat Clin Pract Neurol 2008;4:226–232.
10. Johnson JK, Head E, Kim R, Starr A, Cotman CW. Clinical and pathological evidence for a frontal variant of Alzheimer disease. Arch Neurol 1999;56:1233.

11. Blennerhassett R, Lillo P, Halliday GM, Hodges JR, Kril JJ. Distribution of pathology in frontal variant Alzheimer's disease. J Alzheimers Dis 2014;39:63–70.
12. Singleton AEH, Pijnenburg YAL, Sudre CH, et al. Investigating the clinico-anatomical dissociation in the behavioral variant of Alzheimer's disease. MedRxiv 2019; Available at: medrxiv.org/content/10.1101/19006676v1. Accessed April 8, 2020.
13. La Joie R, Visani AV, Baker SL, et al. Prospective longitudinal atrophy in Alzheimer's disease correlates with the intensity and topography of baseline tau-PET. Sci Transl Med 2020;12:1–13.
14. Ossenkoppele R, Schonhaut DR, Schöll M, et al. Tau PET patterns mirror clinical and neuroanatomical variability in Alzheimer's disease. Brain 2016;139:1551–1567.
15. Rascovsky K, Hodges JR, Knopman D, et al. Sensitivity of revised diagnostic criteria for the behavioral variant of frontotemporal dementia. Brain 2011;134:2456–2477.
16. Gorno-Tempini ML, Hillis AE, Weintraub S, et al. Classification of primary progressive aphasia and its variants. Neurology 2011;76:1006–1014.
17. Crutch SJ, Schott JM, Rabinovici GD, et al. Consensus classification of posterior cortical atrophy. Alzheimers Dement 2017;13:870–884.
18. Hachinski VC, Iliff LD, Zilhka E, et al. Cerebral blood flow in dementia. Arch Neurol 1975;32:632–637.
19. Robert PH, Clairet S, Benoit M, et al. The apathy inventory: assessment of apathy and awareness in Alzheimer's disease, Parkinson's disease and mild cognitive impairment. Int J Geriatr Psychiatry 2002;17:1099–1105.
20. McKhann G, Drachman D, Folstein M, et al. Clinical diagnosis of Alzheimer's disease: report of the NINCDS-ADRDA Work Group under the auspices of Department of Health and Human Services Task Force on Alzheimer's disease. Neurology 1984;34:939.
21. Murray ME, Graff-Radford NR, Ross OA, et al. Neuropathologically defined subtypes of Alzheimer's disease with distinct clinical characteristics: a retrospective study. Lancet Neurol 2011;10:785–796.
22. Therriault J, Benedet AL, Pascoal TA, et al. Association of apolipoprotein E ε4 with medial temporal tau independent of amyloid-β. JAMA Neurol 2020;77:470–479.
23. Saykin AJ, Shen L, Yao X, et al. Genetic studies of quantitative MCI and AD phenotypes in ADNI: progress, opportunities, and plans. Alzheimers Dement 2015;11:792–814.
24. Pascoal TA, Shin M, Kang MS, et al. In vivo quantification of neurofibrillary tangles with [18F]MK-6240. Alzheimers Res Ther 2018;10:1–14.
25. Thomas BA, Cuplov V, Bousse A, et al. PETPVC: a toolbox for performing partial volume correction techniques in positron emission tomography. Phys Med Biol 2016; 61:7975–7993.
26. Therriault J, Ng KP, Pascoal TA, et al. Anosognosia predicts default mode network hypometabolism and clinical progression to dementia. Neurology 2018;90:e932–e939.
27. Ashburner J, Friston KJ. Voxel-based morphometry: the methods. Neuroimage 2000; 11:805–821.
28. Therriault J, Benedet AL, Pascoal TA, et al. Determining Amyloid-β positivity using [18 F]AZD4694 PET imaging. J Nucl Med. Epub 2020 Jul 31.
29. Lowe VJ, Wiste HJ, Senjem ML, et al. Widespread brain tau and its association with ageing, Braak stage and Alzheimer's dementia. Brain 2018;141:271–287.
30. Buckley RF, Mormino EC, Rabin JS, et al. Sex differences in the association of global amyloid and regional tau deposition measured by positron emission tomography in clinically normal older adults. JAMA Neurol 2019;76:542–551.
31. Worsley KJ, Taylor JE, Tomaiuolo F, Lerch J. Unified univariate and multivariate random field theory. NeuroImage 2004;23:189–195.
32. Fawcett T. An introduction to ROC analysis. Pattern Recognit Lett 2006;27:861–874.
33. Etkin A, Egner T, Kalisch R. Emotional processing in anterior cingulate and medial prefrontal cortex. Trends Cogn Sci 2011;15:85–93.
34. Stoll FM, Fontanier V, Procyk E. Specific frontal neural dynamics contribute to decisions to check. Nat Commun 2016;20:11990.
35. Meder D, Haagensen BN, Hulme O, et al. Tuning the brake while raising the stake: network dynamics during sequential decision-making. J Neurosci 2016;36: 5417–5426.
36. Uddin LQ. Salience processing and insular cortical function and dysfunction. Nat Rev Neurosci 2015;16:55–61.
37. Seeley WW, Crawford R, Rascovsky K, et al. Frontal paralimbic network atrophy in very mild behavioral variant frontotemporal dementia. 2008;65:249–255.
38. Seeley WW, Menon V, Schatzberg AF, et al. Dissociable intrinsic connectivity networks for salience processing and executive control. J Neurosci 2007;27: 2349–2356.
39. Seeley WW, Crawford RK, Zhou J, Miller BL, Greicius MD. Neurodegenerative diseases target large-scale human brain networks. Neuron 2009;62:42–52.
40. Harrison TM, La Joie R, Maass A, et al. Longitudinal tau accumulation and atrophy in aging and Alzheimer disease. Ann Neurol 2019;85:229–240.
41. Whitwell JL, Dickson DW, Murray ME, et al. Neuroimaging correlates of pathologically defined subtypes of Alzheimer's disease: a case-control study. Lancet Neurol 2012;11:868–877.
42. De Souza LC, Corlier F, Habert MO, et al. Similar amyloid-β burden in posterior cortical atrophy and Alzheimer's disease. Brain 2011;134:2036–2043.
43. Lehmann M, Ghosh PM, Madison C, et al. Diverging patterns of amyloid deposition and hypometabolism in clinical variants of probable Alzheimer's disease. Brain 2013; 136:844–858.
44. Miller ZA, Rosenberg L, Santos-Santos MA, et al. Prevalence of mathematical and visuospatial learning disabilities in patients with posterior cortical atrophy. JAMA Neurol 2018;75:728.
45. Miller ZA, Mandelli ML, Rankin KP, et al. Handedness and language learning disability differentially distribute in progressive aphasia variants. Brain 2013;136: 3461–3473.
46. Rabinovici GD, Gatsonis C, Apgar C, et al. Association of amyloid positron emission tomography with subsequent change in clinical management among Medicare beneficiaries with mild cognitive impairment or dementia. JAMA 2019;321:1286–1294.
47. Ossenkoppele R, Rabinovici GD, Smith R, et al. Discriminative accuracy of [18F] flortaucipir positron emission tomography for Alzheimer disease vs other neurodegenerative disorders. JAMA 2018;320:1151–1162.
48. Power MC, Mormino E, Soldan A, et al. Combined neuropathological pathways account for age-related risk of dementia. Ann Neurol 2018;84:10–22.
49. Schneider JA, Arvanitakis Z, Bang W, Bennett DA. Mixed brain pathologies account for most dementia cases in community-dwelling older persons. Neurology 2007;69: 2197–2204.
50. Braak H, Braak E. Staging of Alzheimer's disease-related neurofibrillary changes. Neurobiol Aging 1995;16:271–278.
51. Townley RA, Graff-Radford J, Mantyh WG, et al. Progressive dysexecutive syndrome due to Alzheimer's disease: a description of 55 cases and comparison to other phenotypes. Brain Commun 2020;2;fcaa068.

# Topographic Distribution of Amyloid-β, Tau, and Atrophy in Patients With Behavioral/Dysexecutive Alzheimer Disease

Joseph Therriault, Tharick A. Pascoal, Melissa Savard, et al.

*Neurology* 2021;96;e81-e92 Published Online before print October 22, 2020
DOI 10.1212/WNL.0000000000011081